Eur. Phys. J. D **19**, 157–163 (2002)
DOI: 10.1140/epjd/e20020068

THE EUROPEAN PHYSICAL JOURNAL D
EDP Sciences

Electron-atomic-hydrogen "elastic" scattering in the presence of a laser field

S.-M. Li[1,2,a], J. Chen[2,3], and Z.-F. Zhou[3]

[1] Open Laboratory of Bond Selective Chemistry, Department of Modern Physics, University of Science and Technology of China, P.O. Box 4, Hefei, Anhui 230027, P.R. China
[2] China Center of Advanced Science and Technology (World Laboratory), P.O. Box 8730, Beijing 100080, P.R. China
[3] Department of Modern Physics, University of Science and Technology of China, P.O. Box 4, Hefei, Anhui 230027, P.R. China

Received 18 October 2001 and Received in final form 26 December 2001

Abstract. Laser-assisted electron-atomic-hydrogen "elastic" scattering is studied in the first Born approximation. The initial and final states of projectile electron are described by the Volkov wavefunctions; the dressed state of target described by a time-dependent perturbative wavefunction in soft photon approximation. The laser modified cross-sections are calculated in two distinct geometries for laser polarization either parallel or perpendicular to the incident direction of electron. The numerical results shows that the multiphoton cross-sections oscillate by a few orders over the whole scattering angular region. The results for a parallel geometry oscillate more frequently in the intermediate angles; while the results for a perpendicular geometry oscillate more frequently in the forward and backward angles. At large scattering angles, the sum rule of Kroll and Watson is noticeably violated. The laser modification on summed total cross-section increases with field strength, but decreases with field frequency and polarization deviation from the incident direction.

PACS. 34.50.Rk Laser-modified scattering and reactions – 34.80.-i Electron scattering – 32.80.Wr Other multiphoton processes – 34.90.+q Other topics in atomic and molecular collision processes and interactions

1 Introduction

Since the pioneer work of Bunkin and Fedorov [1], laser-assisted electron-atom collisions have been extensively studied [2–4]. The laser-assisted "elastic" scattering (free-free transition) is the simplest one of this kind of collisions. In the theoretical treatment of the free-free process, the atomic target was initially described by a static potential but starting with the work of Gersten and Mittleman [5] the dressing of target was taken into account, and the radiation-atom interaction was treated perturbatively. Along the same lines, work was published by Zon [6], Berlin and Zon [7], Joachain and co-workers [8–10], Dubois *et al.* [11,12], and other authors [13–17]. The experimental reports on this process may be found in the work of Weingartshofer *et al.* [18–20] and Wallbank *et al.* [21–25]. Although much progress has been achieved during the past decades in understanding many aspects of this process, the effects on one another of such new insights are not always apparent in the literature. In fact, the laser-assisted scattering is a time-dependent problem, an united exact treatment is generally not possible. Various models or approximations are developed to study different aspect of the problem. For nonresonant field case, a perturbative treatment to the dressed state of target needs to take an infinite number of coupled states into account, thus greatly increases the computer labor. In most calculations, only a few multiphoton processes are considered and only the cross-section behavior in a small angular range is discussed.

In this paper, the "elastic" collision between an electron and an atomic hydrogen in the presence of an intense nonresonant laser field is investigated in the first Born approximation (FBA) with using a dressed wave function of target obtained as a perturbative solution of time-dependent Schrödinger equation in velocity gauge, and simplified in soft-photon approximation [26]. A large number of multiphoton processes are taken into account, and the calculation covers the whole angular range. In Section 2, the theory is set up. In Section 3, the laser modified cross-sections and their dependence on laser parameters are discussed. Section 4 contains conclusions. The atomic unit $\hbar = m = e = 1$ will be used through out.

2 Theory

Consider the electron-atomic-hydrogen "elastic" scattering embedded in a spatially homogeneous laser background. The laser is described as a linearly polarized

[a] e-mail: lism@ustc.edu.cn or e-mail: enoch@126.com

classical electromagnetic field by vector potential

$$\mathbf{A}(t) = \mathbf{A}_0 \cos\omega t \tag{1}$$

or electric field strength

$$\boldsymbol{\mathcal{E}}(t) = \boldsymbol{\mathcal{E}}_0 \sin\omega t \tag{2}$$

where $\boldsymbol{\mathcal{E}}_0 = (\omega/c)\mathbf{A}_0$ (c is the velocity of light in vacuum). We choose the target nucleus as the origin of the coordinate system which is assumed infinitely massive, set z-axis along the incident direction of the projectile electron, and the zx-plane is defined by the polarization vector $\boldsymbol{\mathcal{E}}_0$ and the incident momentum $\mathbf{k}_\mathrm{i}$. The positions of incident and bound electrons are labeled by $\mathbf{r}_0$ and $\mathbf{r}_1$ respectively.

In FBA the scattering matrix for the direct free-free transition is

$$S^\mathrm{dir} = -\mathrm{i}\int_{-\infty}^{\infty} \mathrm{d}t \Big\langle \chi_{\mathbf{k}_\mathrm{f}}(\mathbf{r}_0,t)\psi_0^\mathrm{H}(\mathbf{r}_1,t)\left|-\frac{1}{r_0}+\frac{1}{r_{10}}\right| \times \chi_{\mathbf{k}_\mathrm{i}}(\mathbf{r}_0,t)\psi_0^\mathrm{H}(\mathbf{r}_1,t)\Big\rangle \tag{3}$$

where $\mathbf{r}_{10} = \mathbf{r}_1 - \mathbf{r}_0$. $\chi_{\mathbf{k}_\mathrm{i}}(\mathbf{r}_0,t)$ and $\chi_{\mathbf{k}_\mathrm{f}}(\mathbf{r}_0,t)$ are respectively the initial and final states of free electron. They may generally be described by the Volkov wavefunction [27,28],

$$\chi_{\mathbf{k}}(\mathbf{r}_0,t) = (2\pi)^{-3/2}\exp\left\{\mathrm{i}\left[\mathbf{k}\cdot\mathbf{r}_0 - \mathbf{k}\cdot\boldsymbol{\alpha}_0\sin\omega t - Et - \frac{1}{2c^2}\int_{-\infty}^{t} A^2(t')\mathrm{d}t'\right]\right\} \tag{4}$$

where $\boldsymbol{\alpha}_0 = \boldsymbol{\mathcal{E}}_0/\omega^2$ and $E = k^2/2$. $\psi_0^\mathrm{H}(\mathbf{r}_1,t)$ is the dressed ground state of target, which is obtained by the time-dependent perturbation theory [26]

$$\psi_0^\mathrm{H}(\mathbf{r}_1,t) = \left\{1 - \left[\mathrm{i}\cos\omega t + \frac{\omega}{\bar{\omega}_\mathrm{H}}\sin\omega t\right]\frac{1}{\omega}\boldsymbol{\mathcal{E}}_0\cdot\mathbf{r}_1\right\}\phi_0^\mathrm{H}(\mathbf{r}_1) \times \exp\left\{-\mathrm{i}\left[W_0^\mathrm{H}t + \frac{1}{2c^2}\int_{-\infty}^{t}\mathrm{d}t' A^2(t')\right]\right\} \tag{5}$$

in which $W_0^\mathrm{H} = 1/2$ a.u. is the ground state energy of atomic hydrogen, $\bar{\omega}_\mathrm{H} = 4/9$ a.u. the average excitation energy for the dressed ground state [29]. $\phi_0^\mathrm{H}(\mathbf{r}_1)$ is the "bare" ground state,

$$\phi_0^\mathrm{H}(\mathbf{r}_1) = \frac{1}{\sqrt{\pi}}\mathrm{e}^{-\mu r_1},\ (\mu = 1). \tag{6}$$

Substitute equations (4–6) into equation (3), and perform the time integration we obtain,

$$S^\mathrm{dir} = \mathrm{i}(2\pi)^{-1}\sum_{l=-\infty}^{\infty} f_l^\mathrm{dir}\,\delta(E_\mathrm{f} - E_\mathrm{i} + l\omega) \tag{7}$$

in which

$$f_l^\mathrm{dir} = 2J_l(\mathbf{q}\cdot\boldsymbol{\alpha}_0)\frac{[(q^2+4\mu^2)^2 - 16\mu]}{(q^2+4\mu^2)^2} - \frac{256}{\bar{\omega}_\mathrm{H}}J_l'(\mathbf{q}\cdot\boldsymbol{\alpha}_0)\frac{\boldsymbol{\mathcal{E}}_0\cdot\mathbf{q}}{q^2(q^2+4\mu^2)^3} \tag{8}$$

where $\mathbf{q} = \mathbf{k}_\mathrm{f} - \mathbf{k}_\mathrm{i}$ is the momentum transfer of projectile. In obtaining equation (8), we have used the following formulas for Bessel functions [30],

$$\mathrm{e}^{\mathrm{i}y\sin u} = \sum_{l=-\infty}^{\infty} J_l(y)\mathrm{e}^{\mathrm{i}lu} \tag{9}$$

and

$$J_{l-1}(y) - J_{l+1}(y) = 2J_l'(y). \tag{10}$$

The first term on the right-hand side of equation (8), called "electronic", describes the scattering of a Volkov electron by the undressed atom; the other one, called "atomic", occurs as a result of the dressing effect of target [14].

In the same way, we may calculate the exchange scattering matrix,

$$S^\mathrm{exc} = -\mathrm{i}\int_{-\infty}^{\infty}\mathrm{d}t\Big\langle \chi_{\mathbf{k}_\mathrm{f}}(\mathbf{r}_1,t)\psi_0^\mathrm{H}(\mathbf{r}_0,t)\left|-\frac{1}{r_0}+\frac{1}{r_{10}}\right| \times \chi_{\mathbf{k}_\mathrm{i}}(\mathbf{r}_0,t)\psi_0^\mathrm{H}(\mathbf{r}_1,t)\Big\rangle. \tag{11}$$

Evaluating the time integration yields,

$$S^\mathrm{exc} = \mathrm{i}(2\pi)^{-1}\sum_{l=-\infty}^{\infty} f_l^\mathrm{exc}\,\delta(E_\mathrm{f} - E_\mathrm{i} + l\omega) \tag{12}$$

in which

$$f_l^\mathrm{exc} = 4\nu\Bigg\{J_l(\mathbf{q}\cdot\boldsymbol{\alpha}_0) + \left[\frac{l}{\omega\mathbf{q}\cdot\boldsymbol{\alpha}_0}J_l(\mathbf{q}\cdot\boldsymbol{\alpha}_0) + \frac{1}{\bar{\omega}_\mathrm{H}}J_l'(\mathbf{q}\cdot\boldsymbol{\alpha}_0)\right]\boldsymbol{\mathcal{E}}_0\cdot\frac{\partial}{\partial\mathbf{k}_\mathrm{i}} - \left[\frac{l}{\omega\mathbf{q}\cdot\boldsymbol{\alpha}_0}J_l(\mathbf{q}\cdot\boldsymbol{\alpha}_0) - \frac{1}{\bar{\omega}_\mathrm{H}}J_l'(\mathbf{q}\cdot\boldsymbol{\alpha}_0)\right]\boldsymbol{\mathcal{E}}_0\cdot\frac{\partial}{\partial\mathbf{k}_\mathrm{f}}\Bigg\} \times\left[\frac{4}{(k_\mathrm{i}^2+\mu^2)(k_\mathrm{f}^2+\nu^2)^2} - \mu\int_0^1 s(1-s)\frac{15\Gamma^4+14\Gamma^2\Lambda^2+3\Lambda^4}{\Gamma^5(\Gamma^2+\Lambda^2)^3}\mathrm{d}s\right] \tag{13}$$

where $\mu = \nu = 1$, and

$$\Gamma = \left[\mu^2 s + \nu^2(1-s) + |\mathbf{k}_\mathrm{f} - \mathbf{k}_\mathrm{i}|^2 s(1-s)\right]^{1/2} \tag{14}$$

$$\boldsymbol{\Lambda} = s\mathbf{k}_\mathrm{i} + (1-s)\mathbf{k}_\mathrm{f} \tag{15}$$

(see the Appendix). In equation (13), the terms multiplied by $J_l(\mathbf{q}\cdot\boldsymbol{\alpha}_0)$ are "electronic", the terms multiplied by $J_l'(\mathbf{q}\cdot\boldsymbol{\alpha}_0)$ "atomic".

The differential cross-section accompanying l photons exchanged between the electron-atom system and the laser background is,

$$\frac{\mathrm{d}\sigma_l}{\mathrm{d}\Omega} = \frac{k_\mathrm{f}}{k_\mathrm{i}}\left(\frac{1}{4}\left|f_l^\mathrm{dir} + f_l^\mathrm{exc}\right|^2 + \frac{3}{4}\left|f_l^\mathrm{dir} - f_l^\mathrm{exc}\right|^2\right). \tag{16}$$

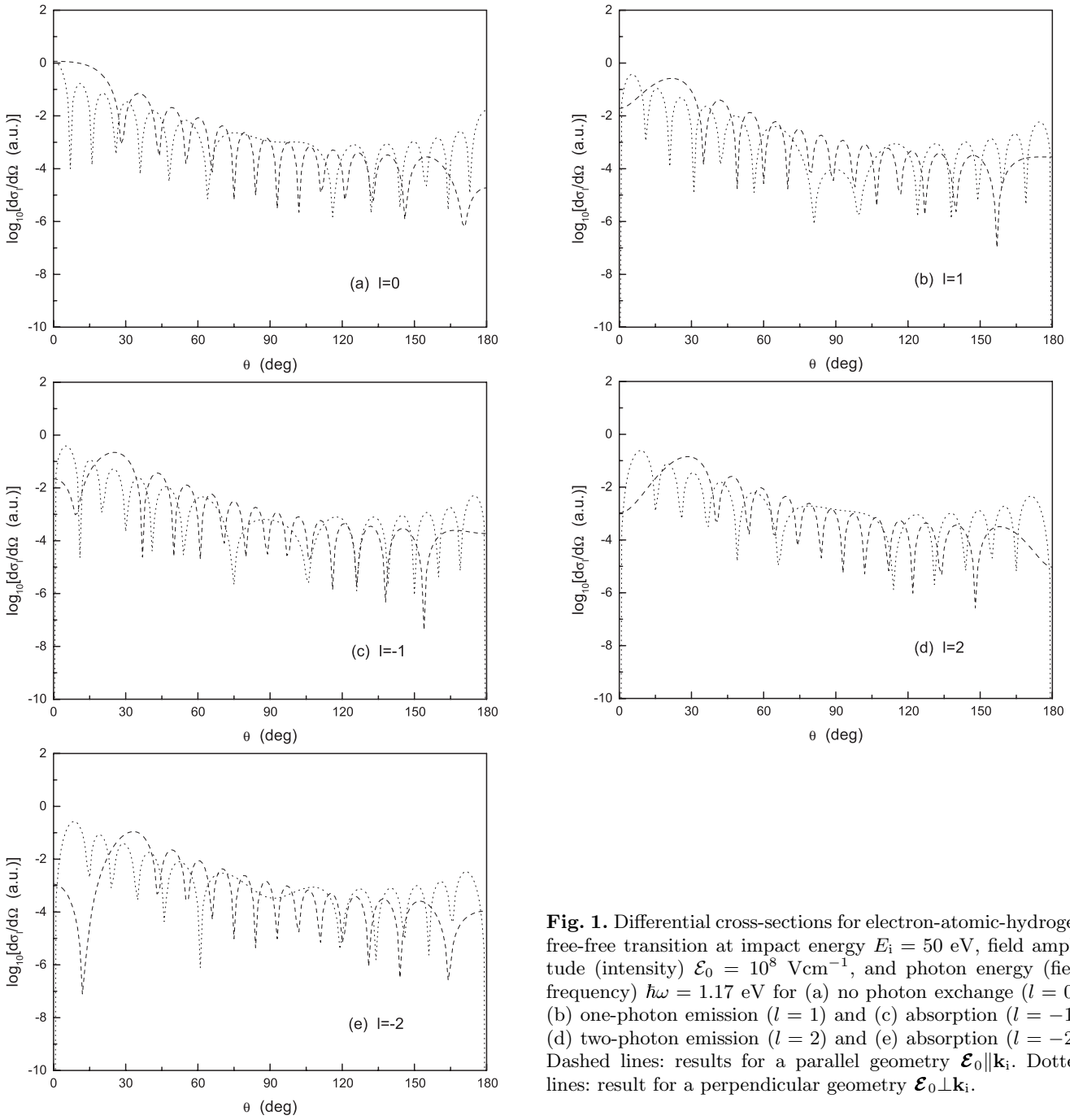

Fig. 1. Differential cross-sections for electron-atomic-hydrogen free-free transition at impact energy $E_\mathrm{i} = 50$ eV, field amplitude (intensity) $\mathcal{E}_0 = 10^8$ Vcm^{-1}, and photon energy (field frequency) $\hbar\omega = 1.17$ eV for (a) no photon exchange ($l = 0$), (b) one-photon emission ($l = 1$) and (c) absorption ($l = -1$), (d) two-photon emission ($l = 2$) and (e) absorption ($l = -2$). Dashed lines: results for a parallel geometry $\boldsymbol{\mathcal{E}}_0 \| \mathbf{k}_\mathrm{i}$. Dotted lines: result for a perpendicular geometry $\boldsymbol{\mathcal{E}}_0 \perp \mathbf{k}_\mathrm{i}$.

Sum over all the multiphoton cross-sections we gain the summed differential cross-section,

$$\frac{\mathrm{d}\sigma}{\mathrm{d}\Omega} = \sum_{l=-\infty}^{+\infty} \frac{\mathrm{d}\sigma_l}{\mathrm{d}\Omega}\,. \tag{17}$$

Integrating over the solid angle yields the summed total cross-section for the laser-assisted "elastic" scattering,

$$\sigma = \int \frac{\mathrm{d}\sigma}{\mathrm{d}\Omega}\mathrm{d}\Omega. \tag{18}$$

3 Results and discussion

In Figure 1 we display the differential cross-section accompanying $l = 0, \pm 1, \pm 2$ photons exchanged between the electron-atom system and the radiation field, for impact energy $E_\mathrm{i} = 50$ eV, field amplitude $\mathcal{E}_0 = 10^8$ Vcm^{-1}, and photon energy (field frequency) $\hbar\omega = 1.17$ eV. We are working in two distinct geometries for the laser polarization vector $\boldsymbol{\mathcal{E}}_0$ either parallel or perpendicular to the incident momentum $\mathbf{k}_\mathrm{i}$. The features of these graphs are more or less the same. Each cross-section oscillates by a few orders over the whole scattering angular range. However,

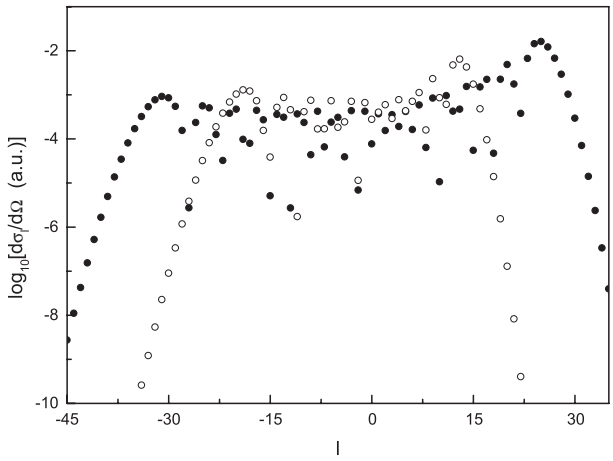

Fig. 2. Values of differential cross-sections at a scattering angle $\theta = 120^\circ$ and an azimuth angle $\phi = 0^\circ$ (the zx-plane is defined by the polarization vector $\boldsymbol{\mathcal{E}}_0$ and the incident momentum $\mathbf{k}_\mathrm{i}$) for each multiphoton process. The impact energy and laser parameters are the same as in Figure 1. Solid circles: result for $\boldsymbol{\mathcal{E}}_0 \| \mathbf{k}_\mathrm{i}$. Open circles: result for $\boldsymbol{\mathcal{E}}_0 \perp \mathbf{k}_\mathrm{i}$.

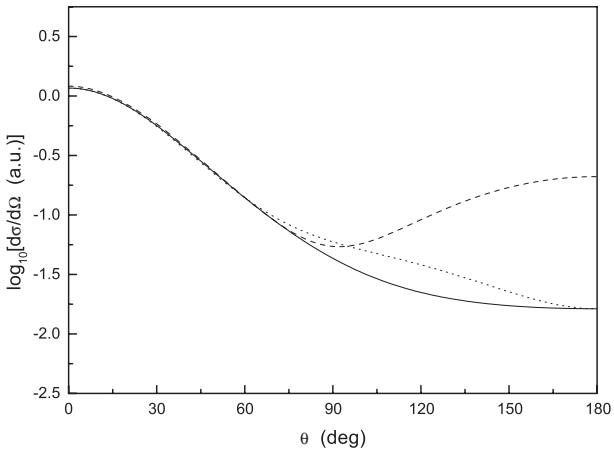

Fig. 3. Summed differential cross-section at azimuth angle $\phi = 0^\circ$. The impact energy and laser parameters are the same as in Figure 1. Solid line: result for laser-free. Dashed line: result for $\boldsymbol{\mathcal{E}}_0 \| \mathbf{k}_\mathrm{i}$. Dotted line: result for $\boldsymbol{\mathcal{E}}_0 \perp \mathbf{k}_\mathrm{i}$.

there is a significant difference between the results of both geometries in each graph: the cross-section for a parallel geometry oscillate more frequently in the intermediate angles, and its envelop (not drown in each graph) declines with scattering angle increasing; in contrast, the results for a perpendicular geometry oscillate more frequently at the forward and backward angles, and its envelop (not present in each graph) rise after $\theta = 90^\circ$. In fact at the impact energy considered, the direct amplitude dominates the exchange amplitude. The Bessel function $J_l(\mathbf{q}\cdot\boldsymbol{\alpha}_0)$ and its derivative $J_l'(\mathbf{q}\cdot\boldsymbol{\alpha}_0)$ appearing in the direct amplitude of equation (8) is responsible for the cross-section oscillation. For a parallel polarization geometry, the argument of Bessel function changes slowly against the scattering angle in the forward and backward direction, which cause the cross-sections oscillating slowly; in medium angular range the argument varies rapidly, and leads to the rapid oscillation of cross-section at mediate angles. For a perpendicular polarization geometry, the situation is opposite: the argument of Bessel functions varies rapidly at small and large angles, but slowly at intermediate angles, thus leads to the opposite feature in the perpendicularly polarized cross-sections.

Figure 2 shows the values of differential cross-sections in both geometries against the exchanged photon number at a scattering angle $\theta = 120^\circ$, and an azimuth angle $\phi = 0^\circ$. Positive l corresponds to the case when the electron-atom system emits photons to the laser field (the stimulated Bremsstrahlung), while negative l is associate with photon absorption (the inverse Bremsstrahlung). We find that for both geometries, the inverse Bremsstrahlung processes dominate the bremsstrahlung processes. The results for a parallel geometry cover a relatively wider regime of photon numbers than that for a perpendicular geometry. According to the asymptotic expression of Bessel function at large argument $J_l(l/\cosh a) \approx \mathrm{e}^{l\tanh a - la}/\sqrt{2l\pi\tanh a}$ [30], $J_l(x)$ declines with l when l is large enough. The greater the argument, the more rapidly the Bessel function declines. At the scattering angle considered, the argument of $J_l(\mathbf{q}\cdot\boldsymbol{\alpha}_0)$ acquires a greater value in a perpendicular polarization geometry than in a parallel geometry, therefore the cross-section for a perpendicular geometry declines more rapidly for large l.

In Figure 3 we give the summed differential cross-sections. The summed cross-sections for both geometries are hardly affected by laser at small scattering angles, but highly modified at large angles. This suggests that at large angles, the sum rule of Kroll and Watson [31,32] is violated. As a matter of fact, during such a scattering process, the state of target remains unchanged after the collision happens. The target is no more a "spectator". Without the presence of such a "spectator", a free electron can not exchange energy with the radiation field. At small scattering angle (or large impact parameter), the state of projectile electron is not very strongly affected by the target, and exchange less energy with the field background, thus the contribution of laser modification on cross-section at small angle is small. Large angle scattering is associated with the projectile acceleration by the Coulomb field of target. During the acceleration processes, the projectile may exchange a considerable amount of photons with the laser field. The laser oscillation tends to keep the projectile around the target and enhance the scattering probability backward, thus the summed cross-section is notably enhanced at large angles. For a perpendicular geometry, apart from the above effect, the field also deflects the incident electron from aiming at the target, thus the cross-section enhancement in a perpendicular geometry is not as significant as that in a parallel geometry.

When the laser polarization deviates from the incident direction, the axial symmetry of the collision process is broken, thus the cross-sections becomes azimuth-dependent. Figure 4 shows the summed cross-section of the perpendicular geometry *versus* the azimuth angle.

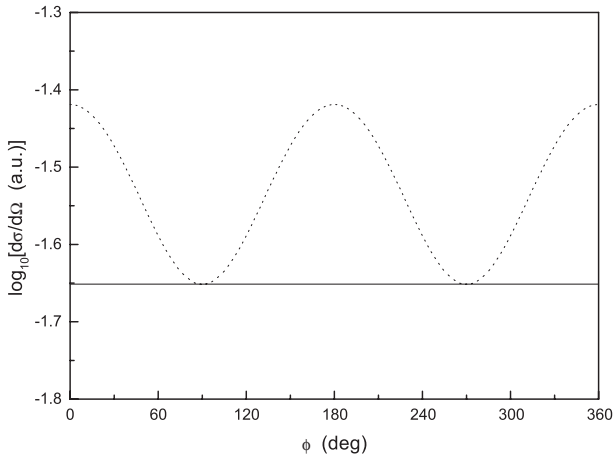

Fig. 4. Summed differential cross-section against azimuth angle at scattering angle $\theta = 120°$. The impact energy and laser parameters are the same as in Figure 1. Solid line: result for laser-free. Dotted line: result for $\boldsymbol{\mathcal{E}}_0 \perp \mathbf{k}_\mathrm{i}$.

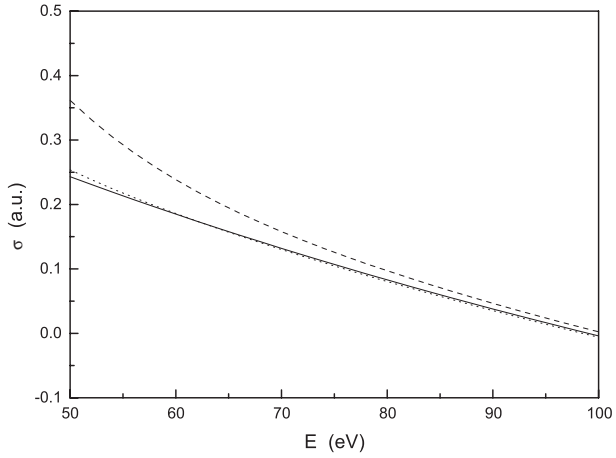

Fig. 5. Summed total cross-sections for laser-assisted "elastic" scattering. The laser parameters are the same as in Figure 1. Solid line: result for laser-free. Dashed line: result for $\boldsymbol{\mathcal{E}}_0 \| \mathbf{k}_\mathrm{i}$. Dotted line: result for $\boldsymbol{\mathcal{E}}_0 \perp \mathbf{k}_\mathrm{i}$.

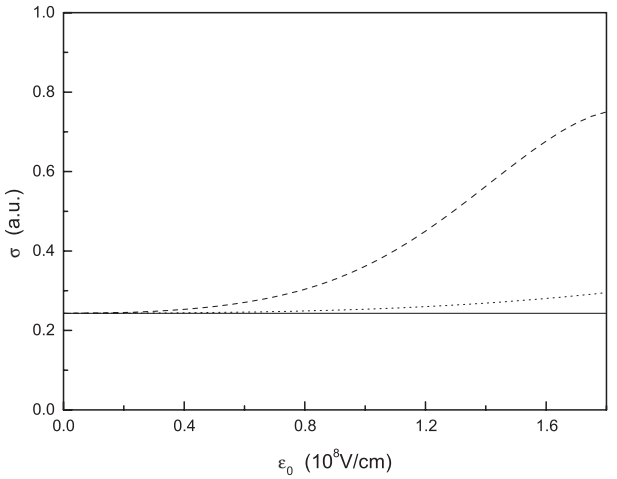

Fig. 6. Summed total cross-sections against field strength for impact energy $E_\mathrm{i} = 50$ eV and photon energy $\hbar\omega = 1.17$ eV. Solid line: result for laser-free. Dashed line: result for $\boldsymbol{\mathcal{E}}_0 \| \mathbf{k}_\mathrm{i}$. Dotted line: result for $\boldsymbol{\mathcal{E}}_0 \perp \mathbf{k}_\mathrm{i}$.

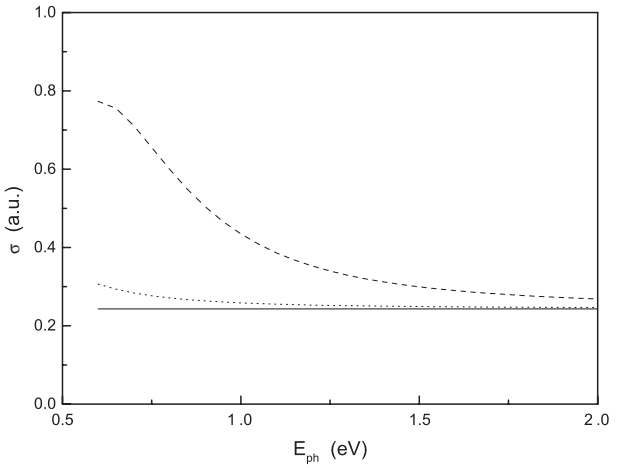

Fig. 7. Summed total cross-sections against laser photon energy $E_\mathrm{ph} = \hbar\omega$ for impact energy $E_\mathrm{i} = 50\,\mathrm{eV}$ and field amplitude $\mathcal{E}_0 = 10^8\ \mathrm{Vcm}^{-1}$. Solid line: result for laser-free. Dashed line: result for $\boldsymbol{\mathcal{E}}_0 \| \mathbf{k}_\mathrm{i}$. Dotted line: result for $\boldsymbol{\mathcal{E}}_0 \perp \mathbf{k}_\mathrm{i}$.

Since the laser-assisted collision process is symmetric about the zx-plane, the polarization dependence is periodic. When the momentum of scattered electron is in the zx-plane ($\phi = 0°, 180°$), the cross-section is maximized; when $\mathbf{k}_\mathrm{f}$ perpendicular to the zx-plane ($\phi = 90°, 270°$), the result is minimized. This is because that when electron in the plane of $\boldsymbol{\mathcal{E}}_0$ and $\mathbf{k}_\mathrm{i}$, its state is most efficiently modified by the field.

Figure 5 shows the summed total cross-section for the laser-assisted "elastic" scattering. The total cross-section enhancement is mainly contributed by the differential cross-section of large angles. Since the laser-enhancement for a parallel geometry is greater than that for a perpendicular geometry, the total cross-section for the former case is higher than that for the latter case.

Figures 6–8 respectively demonstrate the dependence of summed total cross-sections on field amplitude (intensity), photon energy (laser frequency), and orientation of polarization (assume that the orientation of $\boldsymbol{\mathcal{E}}_0$ varies in the zx-plane). The stronger the laser, the more likely the colliding system exchange photons with the filed, thus the more the cross-section enhancement. The lower the frequency, the more the average contribution of laser to the cross-section enhancement (the resonance case is not included). As we expect, the more the polarization deviated from the incident direction, the less likely the scattering is assisted, thus the result reaches the maximum at a parallel geometry ($\Theta = 0°, 180°$), but gains its minimum at a perpendicular geometry ($\Theta = 90°, 270°$).

4 Conclusions

In the present work we have calculated the multiphoton cross-sections and the summed cross-sections for the

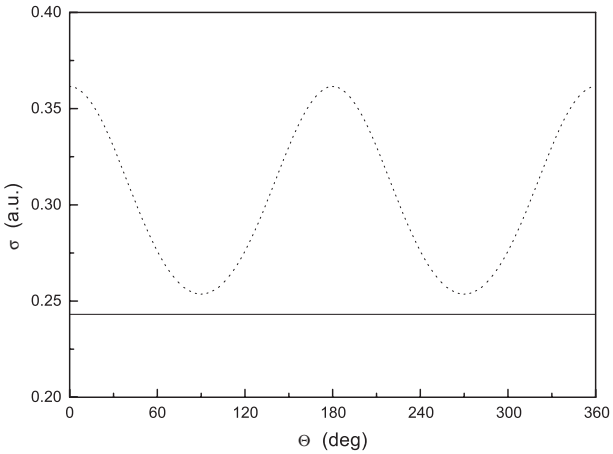

Fig. 8. The dependence of summed total cross-sections on polarization orientation (assume that the orientation of $\boldsymbol{\mathcal{E}}_0$ varies in the zx-plane). The impact energy and laser parameters are the same as in Figure 1. Solid line: result for laser-free. Dashed line: result for $\boldsymbol{\mathcal{E}}_0 \| \mathbf{k}_\mathrm{i}$. Dotted line: result for $\boldsymbol{\mathcal{E}}_0 \perp \mathbf{k}_\mathrm{i}$.

laser-assisted electron-atomic-hydrogen "elastic" scattering in the whole angular regime with using of a simplified dressed wave function of target which does not involve the space-dependent gauge factor and the infinite summation over the coupled atomic states. Such a calculation is much more accurate in describing the collision dynamics than treating the atom as a model potential [33,34] although the latter may be used for estimation. Due to the time-dependent nature of the laser-assisted process, both the electron-electron and electron-nucleus interactions are taken into account. When laser polarization deviates from the incident direction of projectile, the axial symmetry of the scattering process is broken down, and the summed differential cross-section for a perpendicular geometry becomes azimuth angle dependent. The numerical results show that during such a laser-assisted "elastic" collision, the electron-atom system may exchange a great number of photons with the laser background. Each multiphoton cross-section oscillates by a few orders over the whole scattering angular region. For a parallel polarization geometry, the result oscillates more frequently in the medium angular range than in the forward and backward angles; while for a perpendicular geometry, the oscillation feature is opposite. At large scattering angles, the sum rule of Kroll and Watson is violated. This suggests that at lower impact energy, one may use a strong laser field to enhance the backward angular distribution which is usually more difficult to detect in the usual laser-free scattering. When the electric vector of laser is parallel to the incident direction of electron, the cross-section is most efficiently enhanced. The total cross-section is significantly modified in the low energy regime. The more intense the laser, the more the cross-section is enhanced; the lower the field frequency, the more the cross-section enhancement.

At present, almost all the free-free experiments have used CO_2 laser as radiation field ($\hbar\omega = 0.117$ eV) and used argon as target. For such cases, the Kroll-Watson sum rule is valid in general. Extension to use of powerful Nd-YAG lasers ($\hbar\omega = 1.17$ eV) now available is contemplated by several experiment groups. An experimental program to study the free-free collision from atomic hydrogen will require the collaboration of several experimental groups if they are to be successful [35]. Such experiments are necessary to test the theory and our understanding of laser-modified electron scattering.

This work is supported by the National Natural Science Foundation of China under Grant Numbers 10074060 and 10075043.

Appendix: Derivation of the exchange amplitude of equation (13)

After working out the time integration in equation (11), we obtain the exchange amplitude associated with the transfer of l photons,

$$f_l^{\mathrm{exc}} = -\Bigg\{ J_l(\mathbf{q}\cdot\boldsymbol{\alpha}_0) + \left[\frac{l}{\omega\mathbf{q}\cdot\boldsymbol{\alpha}_0} J_l(\mathbf{q}\cdot\boldsymbol{\alpha}_0) + \frac{1}{\bar{\omega}_\mathrm{H}} J_l'(\mathbf{q}\cdot\boldsymbol{\alpha}_0)\right] \boldsymbol{\mathcal{E}}_0\cdot\frac{\partial}{\partial\mathbf{k}_\mathrm{i}} - \left[\frac{l}{\omega\mathbf{q}\cdot\boldsymbol{\alpha}_0} J_l(\mathbf{q}\cdot\boldsymbol{\alpha}_0) - \frac{1}{\bar{\omega}_\mathrm{H}} J_l'(\mathbf{q}\cdot\boldsymbol{\alpha}_0)\right] \boldsymbol{\mathcal{E}}_0\cdot\frac{\partial}{\partial\mathbf{k}_\mathrm{f}} \Bigg\} (I_1 + I_2) \tag{A.1}$$

in which I_1 and I_2 are parametric integrals,

$$I_1 = \frac{1}{2\pi^2}\int \mathrm{d}\mathbf{r}_0\mathrm{d}\mathbf{r}_1 \mathrm{e}^{\mathrm{i}\mathbf{k}_\mathrm{i}\cdot\mathbf{r}_0 - \mu r_0}\mathrm{e}^{-\mathrm{i}\mathbf{k}_\mathrm{f}\cdot\mathbf{r}_1 - \nu r_1}\left(-\frac{1}{r_0}\right) \tag{A.2}$$

$$I_2 = \frac{1}{2\pi^2}\int \mathrm{d}\mathbf{r}_0\mathrm{d}\mathbf{r}_1 \mathrm{e}^{\mathrm{i}\mathbf{k}_\mathrm{i}\cdot\mathbf{r}_0 - \mu r_0}\mathrm{e}^{-\mathrm{i}\mathbf{k}_\mathrm{f}\cdot\mathbf{r}_1 - \nu r_1}\frac{1}{r_{10}} \tag{A.3}$$

with differential parameters $\mu = \nu = 1$. In obtaining equation (A.1), we have used the formulae (9, 10), and

$$J_{l-1}(y) + J_{l+1}(y) = \frac{2l}{y} J_l(y) \tag{A.4}$$

for Bessel functions [30].

The integral I_1 in equation (A.2) is in fact a product of two simple three-fold integrals. It is easy to work out to yield,

$$I_1 = -\frac{16\nu}{(k_\mathrm{i}^2 + \mu^2)(k_\mathrm{f}^2 + \nu^2)^2}\,. \tag{A.5}$$

Now lets' consider the integral I_2. Substituting

$$\frac{1}{r_{10}} = \frac{1}{2\pi^2}\int \mathrm{d}\mathbf{p}\frac{\mathrm{e}^{\mathrm{i}\mathbf{p}\cdot(\mathbf{r}_0 - \mathbf{r}_1)}}{r_{10}} \tag{A.6}$$

into equation (A.3), we obtain

$$\begin{aligned} I_2 &= \frac{1}{4\pi^4}\int \mathrm{d}\mathbf{p}\frac{1}{p^2}\int \mathrm{d}\mathbf{r}_0 \mathrm{e}^{-\mathrm{i}(\mathbf{p}-\mathbf{k}_\mathrm{i})\cdot\mathbf{r}_0-\mu r_0} \\ &\quad\times\int \mathrm{d}\mathbf{r}_1 \mathrm{e}^{\mathrm{i}(\mathbf{p}-\mathbf{k}_\mathrm{f})\cdot\mathbf{r}_1-\nu r_1} \\ &= \frac{16\mu\nu}{\pi^2}\int \mathrm{d}\mathbf{p}\frac{1}{p^2}\frac{1}{[\mu^2+(\mathbf{p}-\mathbf{k}_\mathrm{i})^2]^2}\frac{1}{[\nu^2+(\mathbf{p}-\mathbf{k}_\mathrm{f})^2]^2} \\ &= \frac{16\mu\nu}{\pi^2} I_{2,2}(\mu,\nu,\mathbf{k}_\mathrm{i},\mathbf{k}_\mathrm{f},0) \end{aligned} \tag{A.7}$$

where $I_{2,2}(\mu,\nu,\mathbf{k}_\mathrm{i},\mathbf{k}_\mathrm{f},0)$ is the Dalitz integral, which is generally given by [36,37],

$$\begin{aligned} &I_{m,n}(\mu,\nu,\mathbf{k}_\mathrm{i},\mathbf{k}_\mathrm{f},k) = \\ &\int \mathrm{d}\mathbf{p}\frac{1}{p^2-k^2-\mathrm{i}\epsilon}\frac{1}{[\mu^2+(\mathbf{p}-\mathbf{k}_\mathrm{i})^2]^m[\nu^2+(\mathbf{p}-\mathbf{k}_\mathrm{f})^2]^n} \\ &= \frac{(m+n-1)!}{(m-1)!(n-1)!}\int_0^1 s^{m-1}(1-s)^{n-1}L_{m+n}(k,\Gamma,\Lambda)\mathrm{d}s \end{aligned} \tag{A.8}$$

with

$$L_1(k,\Gamma,\Lambda) = \frac{\pi^2\mathrm{i}}{\Lambda}\log\frac{k+\Lambda+\mathrm{i}\Gamma}{k+\Lambda+\mathrm{i}\Gamma} \tag{A.9}$$

$$L_2(k,\Gamma,\Lambda) = -\frac{\pi^2}{\Gamma(k^2-\Gamma^2-\Lambda^2+2\mathrm{i}k\Gamma)} \tag{A.10}$$

$$\cdots$$

$$L_l(k,\Gamma,\Lambda) = -\frac{1}{2(l-1)\Gamma}\frac{\partial L_{l-1}}{\partial\Gamma} \tag{A.11}$$

where Γ and $\boldsymbol{\Lambda}$ are given by equations (14, 15) respectively. In equations (A.9–A.11), set $k=0$, and by successive differentiation with respect to Γ, we gain,

$$L_4(0,\Gamma,\Lambda) = \frac{\pi^2}{24}\frac{15\Gamma^4+10\Gamma^2\Lambda^2+3\Lambda^4}{\Gamma^5(\Gamma^2+\Lambda^2)^3}\,. \tag{A.12}$$

According to equation (A.8),

$$\begin{aligned} I_{2,2}(\mu,\nu,\mathbf{k}_\mathrm{i},\mathbf{k}_\mathrm{f},0) &= 6\int_0^1 s(1-s)L_4(0,\Gamma,\Lambda)\mathrm{d}s \\ &= \frac{\pi^2}{4}\int_0^1 s(1-s)\frac{15\Gamma^4+10\Gamma^2\Lambda^2+3\Lambda^4}{\Gamma^5(\Gamma^2+\Lambda^2)^3}\mathrm{d}s. \end{aligned} \tag{A.13}$$

Substituting it into equation (A.7) yields

$$I_2 = 4\mu\nu\int_0^1 s(1-s)\frac{15\Gamma^4+14\Gamma^2\Lambda^2+3\Lambda^4}{\Gamma^5(\Gamma^2+\Lambda^2)^3}\mathrm{d}s. \tag{A.14}$$

Combine equations (A.1, A.5, A.14), we finally obtain equation (13) for the exchange amplitude.

References

1. F.V. Bunkin, M.V. Fedorov, Sov. Phys. JETP **22**, 844 (1966).
2. P. Francken, C.J. Joachain, J. Opt. Soc. Am. B **7**, 554 (1990).
3. F. Ehlotzky, A. Jaroń, J.Z. Kamiński, Phys. Rep. **297**, 63 (1998).
4. F. Ehlotzky, Phys. Rep. **345**, 175 (2001).
5. J.I. Gersten, M.H. Mittleman, Phys. Rev. A **13**, 123 (1976).
6. B.A. Zon, Sov. Phys. JETP **46**, 65 (1977).
7. E.L. Beilin, B.A. Zon, J. Phys. B **16**, L159 (1983).
8. F.W. Byron Jr, C.J. Joachain, J. Phys. B **17**, L295 (1984).
9. P. Francken, C.J. Joachain, Phys. Rev. A **35**, 1590 (1987).
10. F.W. Byron Jr, P. Francken, C.J. Joachain, J. Phys. B **20**, 5487 (1987).
11. A. Dubois, A. Maquet, S. Jetzke, Phys. Rev. A **34**, 1888 (1986).
12. A. Dubois, A. Maquet, Phys. Rev. A **40**, 4288 (1989).
13. S. Sarkar, M. Chakraboty, Phys. Rev. A **37**, 1456 (1988).
14. D. Khalil, O.El. Akramine, A. Makhoute, A. Maquet, R. Taïb, J. Phys. B **31**, 1115 (1998).
15. A. Cionga, F. Ehlotzky, G. Zloh, Phys. Rev. A **61**, 063417 (2000).
16. M. Bouzidi, A. Makhoute, D. Khalil, A. Maquet, C.J. Joachain, J. Phys. B **34**, 737 (2001).
17. S.T. Zhang, J. Chen, J. Phys. B **34**, 2201 (2001).
18. A. Weingartshofer, J.K. Holmes, J. Sabbagh, E.M. Clarke, H. Kruger, Phys. Rev. Lett. **39**, 269 (1977).
19. A. Weingartshofer, E.M. Clarke, J.K. Holmes, C. Jung, Phys. Rev. A **19**, 2371 (1979).
20. A. Weingartshofer, J.K. Holmes, J. Sabbagh, S.L. Chin, J. Phys. B **16**, 1805 (1983).
21. B. Wallbank, V.W. Connors, J.K. Holmes, A. Weingartshofer, J. Phys. B **20**, L833 (1987).
22. B. Wallbank, V.W. Connors, J.K. Holmes, A. Weingartshofer, J. Phys. B **20**, 6121 (1987).
23. B. Wallbank, J.K. Holmes, Phys. Rev. A **48**, R2515 (1993).
24. B. Wallbank, J.K. Holmes, J. Phys. B **27**, 1221 (1994).
25. B. Wallbank, J.K. Holmes, J. Phys. B **27**, 5405 (1994).
26. S.-M. Li, J. Chen, Z.-F. Zhou, unpublished.
27. D.M. Volkov, Z. Phys. **94**, 250 (1935).
28. S.-M. Li, A.-H. Liu, Z.-F. Zhou, J. Chen, J. Phys. B **33**, 4726 (2000).
29. M. Bhattacharya, C. Sinha, N.C. Sil, Phys. Rev. A **40**, 567 (1989).
30. I.S. Gradshteyn, I.M. Ryzhik, *Tables of Integrals, Series, and Products* (Academic, New York, 1980).
31. M.H. Mittleman, *Introduction to the Theory of Laser-Atom Interactions* (Plenum, New York, 1993).
32. N.M. Kroll, K.M. Watson, Phys. Rev. A **8**, 804 (1973).
33. R. Daniele, G. Ferrante, F. Morales, F. Trombetta, J. Phys. B **19**, L133 (1986).
34. R. Daniele, F. Trombetta, G. Ferrante, P. Cavaliere, F. Morales, Phys. Rev. A **36**, 1156 (1987).
35. N.J. Mason, Rep. Prog. Phys. **56**, 1275 (1993).
36. C.J. Joachain, *Quantum Collision Theory* (North-Holland Publishing, Amsterdam, 1975).
37. R.H. Dalitz, Proc. Roy. Soc. A **206**, 509 (1951).